Supplementary Information

Enhanced Electron Transfer Rates by AC Voltammetry for Ferrocenes Attached to the End of Embedded Carbon Nanofiber Nanoelectrode Arrays

Lateef U Syed, Jianwei Liu, Allan M. Prior, Duy H. Hua, and Jun Li*

Department of Chemistry, Kansas State University, Manhattan, KS 66506

MATERIALS AND METHODS

Materials. The following reagents were used as received: 1-ethyl-3-(3-dimethylaminopropyl) carbodiimide hydrochloride (EDC), *N*-hydrosuccinimide (NHS), sodium hydroxide, potassium chloride (all from Fisher Scietific, Inc) and potassium ferrocyanide (Acros Organics). Aminomethylferrocene ($FcCH_2NH_2$) was prepared by a modification of the reported procedure from the treatment of ferrocenecarboxaldehyde with hydroxylamine and sodium acetate trihydrate in refluxing ethanol and water for 6 h followed by reduction of the resulting oxime (a mixture of cis- and trans-isomers) with lithium aluminum hydride in refluxing tetrahydrofuran (THF) for 2 h [1].

Embedded carbon nanofiber (CNF) nano electrode arrays (NEAs) were made by the method described in previous paper [2]. Briefly, VACNFs were grown on Cr-coated Si substrate using a DC-biased plasma enhanced chemical vapor deposition (PECVD) [3]. A thin nickel film of ~22 nm was used as the catalyst to promote CNF growth. The electric field helped to align the CNF vertically on the substrate surface. Insulation of the bottom Cr metal contact layer and each individual CNF was done by depositing dielectric SiO_2 using chemical vapor deposition (CVD) from vapor-phase tetraethylorthosilicate (TEOS) precursor. Mechanical polishing was applied using 0.3 μm alumina slurry to produce a flat surface. Reactive ion etching (RIE) with a mixture

of CHF_3 and O_2 gases was then performed to selectively etch away desired amount of SiO_2 and expose the tip of a portion of CNFs. The density and length of exposed CNFs were readily controlled by RIE. An O-ring with a 3 mm inside diameter was used between a Teflon electrochemical cell and the electrode to define the area of the working electrode to be exposed in solution. All electrochemical measurements were done with 3-electrode setup with a Pt coil counter electrode and a Ag/AgCl(sat'd KCl) reference electrode.

Functionalization. Glassy carbon electrode (GCE) and CNF NEA were electrochemically etched in 1.0 M NaOH to introduce carboxylic groups, which helps to selectively functionalize Fc moiety $Fc(CH_2)NH_2$ by forming an amide bond facilitated by EDC and NHS. Functionalization procedure was carried out in two steps. In the first step both GCE electrode and NEA were incubated for 2 hrs at room temperature (RT) in aqueous solution of 1 mM EDC and NHS, rinsed both the electrodes with water and in the second step electrodes were incubated with ethanolic solution of 1 mM $FcCH_2NH_2$ for ~16 hrs at RT, after the incubation rinsed both the electrodes with ethanol and then dried in a stream of N_2.

ACV Experiments. As shown in Fig. S1 and Table S1, the electropotential was varied as a staircase waveform from the initial potential (-0.05 V) to the final potential (+0.65 V) with an increment of 5 mV at each step. The step width (i.e. Sample Period) was fixed at 0.5 s. The AC sinewave of 25 mV amplitude was superimposed on the DC staircase ramp (see Fig. S1b, adapted from CHI440A user manual) and the phase-sensitive response of AC signals (current and phase angles) were recorded at each step over at least 5 cycles, which defined that the low limit of the frequency is 10 Hz. The AC current amplitude was plot vs. the electrode potential at each step as AC voltammogram.

Table S1. AC Voltammetry Experimental Parameters

Init E (V)	-0.05
Final E (V)	+0.65
Incr E (mV)	5
Amp (mV)	25
Freq (Hz)	10-10000
Sample Period (sec)	0.5
Quiet time	0 sec

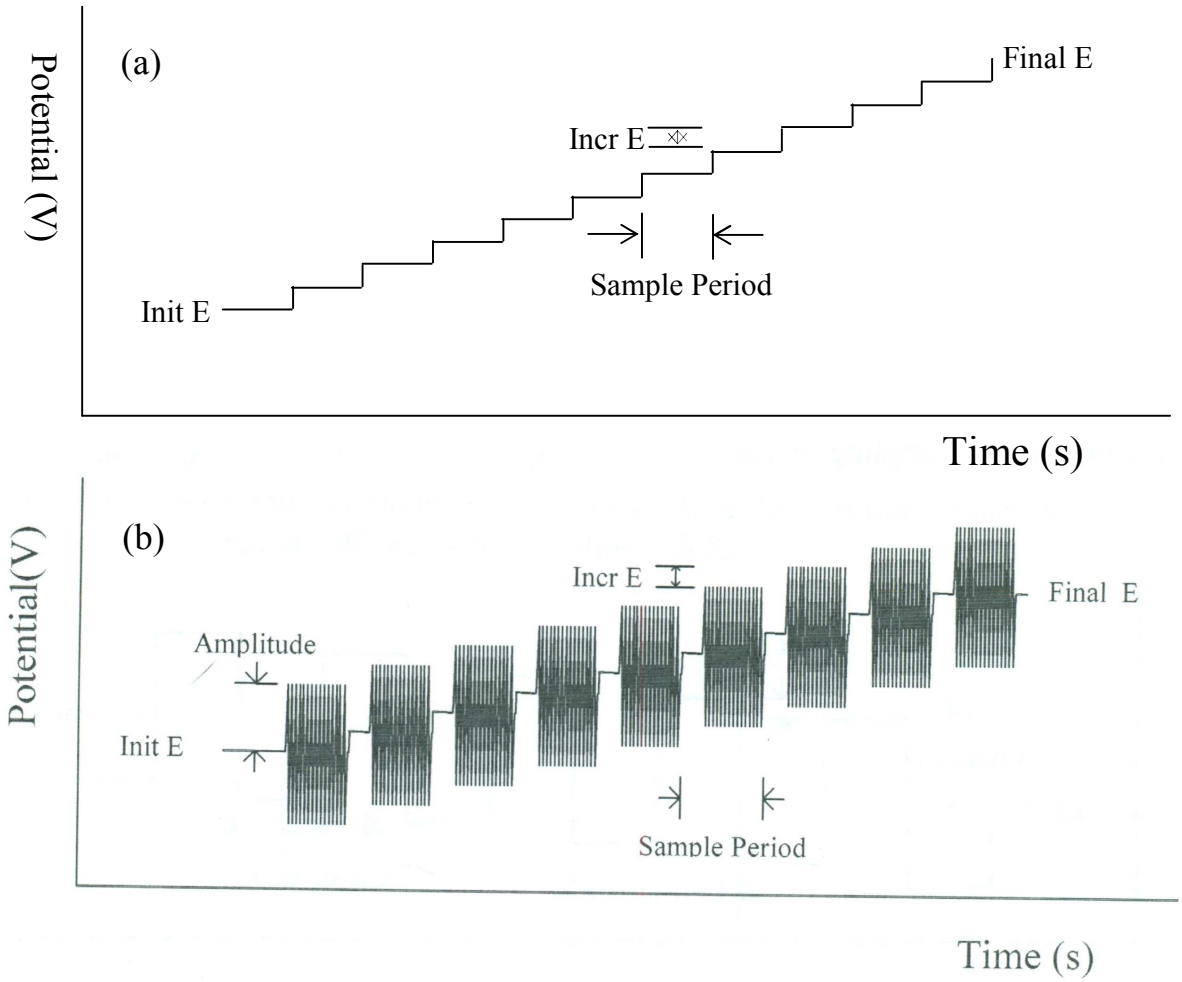

Figure S1: (a) The waveform of the staircase DC potential ramp; (b) Schematic of the AC sinusoidal wave of certain amplitude and frequency superimposed on the staircase DC potential ramp (adapted from CHI440A user manual).

RESULTS AND DISCUSSION

1. Two probe *I-V* measurement of CNF NEA

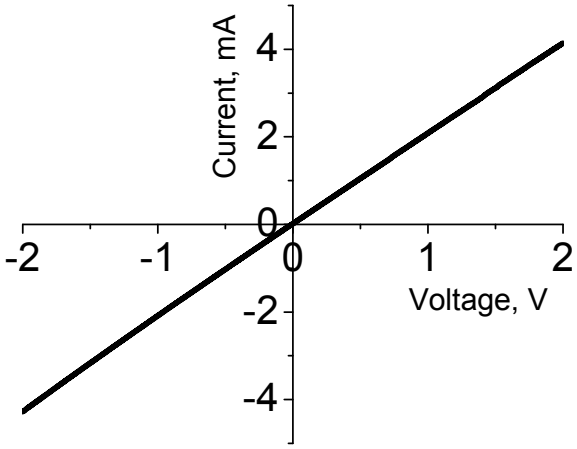

Figure S2. The *I-V* curve of VACNF NEA with a two-terminal measurement.

Figure S2 shows a two terminal *I-V* curve of embedded VACNF NEA measured using CHI440A potentiostat. The two-point contacts with the exposed CNF tips were made using spring loaded gold pins. As seen in Figure S2, the *I-V* curve is linear, consistent with earlier published reports [4,5].

2. CV measurements at the CNF NEA before and after functionalization

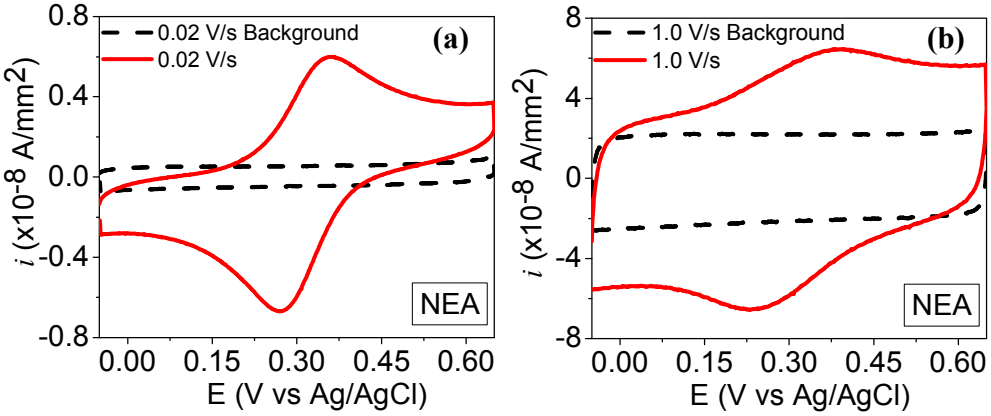

Figure S3. CV measurements of CNF NEA before and after Fc-functionalization in 1.0 M KCl solution at (a) 0.02 and (b) 1.0 V/s scan rate, respectively.

Figure S3 shows CV curves measured before and after Fc-functionalization at the tips of exposed CNFs. In the above figures, it can be clearly observed that the background does not have any tilt, and even at higher scan rates the background increased, but it's not tilted. The faradaic Fc oxidation and reduction signal recorded at both the scan rates is tilted with respect to the background. This might be attributed to the slow electron transfer rate (in case of DC voltammetry) at the CNF NEA due to the unique cup-like graphitic structure of the CNFs, consistent with the discussion made in the paper.

3. ΔE_p vs υ

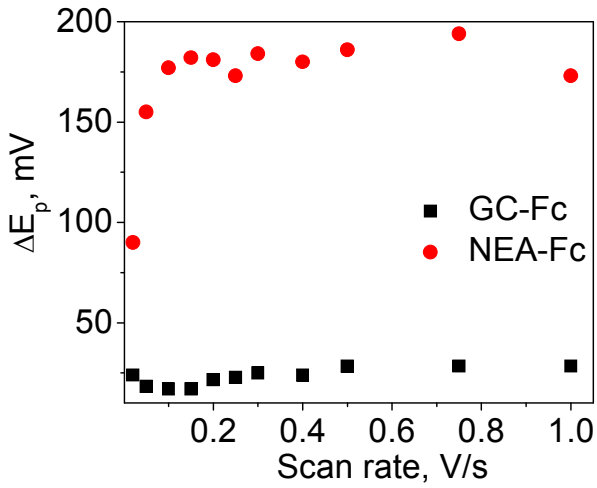

Figure S4. Peak-to-peak splitting (ΔE_p) for Fc-attached to GCE and VACNF NEA as a function of scan rate.

CVs over a range of scan rates (20 mV/s to 1.0 V/s) were recorded after Fc was functionalized to the GCE and the VACNF NEA (see Fig. 2). Figure S4 summarizes a plot of peak-to-peak splitting (of oxidation and reduction peaks) obtained from the CV data of Fig. 2 as a function of scan speed. It can be observed that, at the slow scan rates less than 0.10 V/s, the ΔE_p value increases with the scan rate with that on Fc-functionalized CNF NEA much larger than the GCE.

Whereas, the ΔE_p value on both electrodes is apparently limited by some other processes at DC scan rate larger than 0.10 V/s.

3. ACV experiment data analysis using Creager's approach [6,7]

Figure S5(a) shows ACV signal of a ferrocene-functionalized CNF NEA measured at the highest frequency allowed by the instrument, i.e. 10,000 Hz. As seen in the figure, there is a substantial signal compared to background, where as for GCE it can be seen in Figure 5a that the signal almost levels to background at a frequency of ~1,800 Hz. This clearly shows that CNF NEA has better electron transfer capability. The $(I_p+I_b)/I_b$ vs. log(frequency) shows a plateau at low frequency and drops at high frequency, similar to the observation by Creager et al [6].

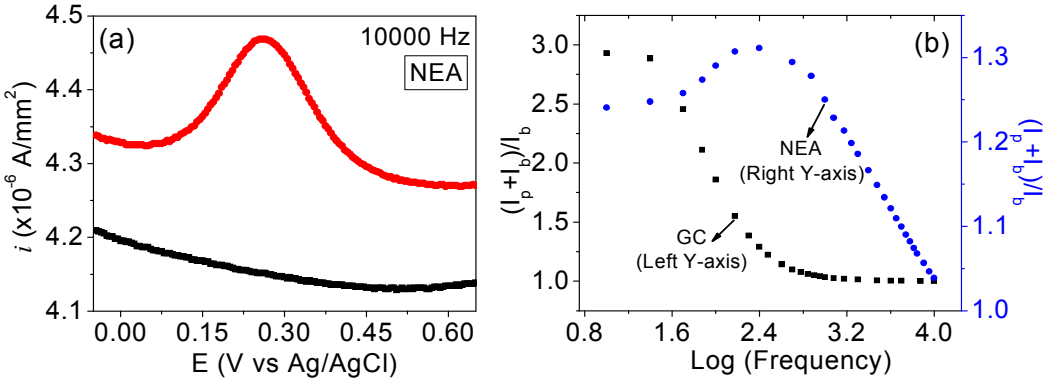

Figure S5. (a) ACV measurement performed on a Fc-functionalized CNF NEA at a AC frequency of 10000 Hz and AC voltage amplitude of 25 mV on the DC staircase ramp from -0.05 to 0.65 V at a scan rate of 20 mV/s in 1 M KCl. (b) Plots of $(I_p+I_b)/I_b$ vs. log(frequency) prepared using ACV data shown in figure 4a-4f for the GC and CNF NEA, in the fashion reported by Creager et al [6].

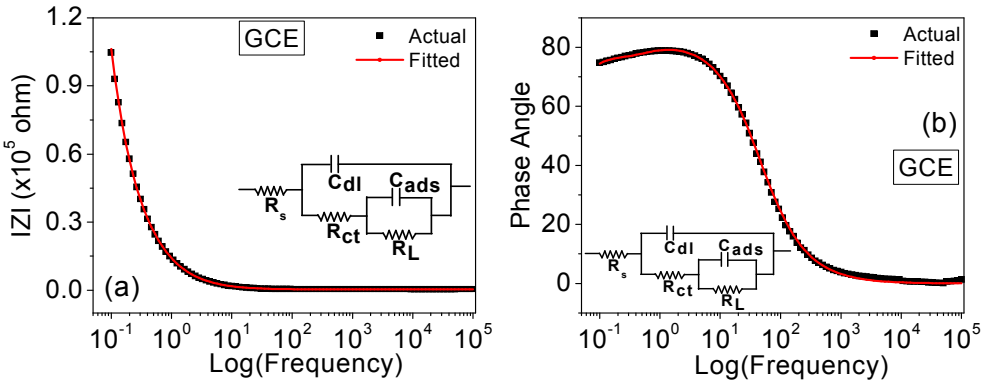

Figure S6. Bode plots of EIS of a GCE functionalized with ferrocene with (a): total impedance vs. log(frequency) and (b): phase angle vs. log(frequency). These are the same EIS data shown in Nyquist plot in Figure 6(a). The insets are the equivalent circuits used to fit the EIS data.

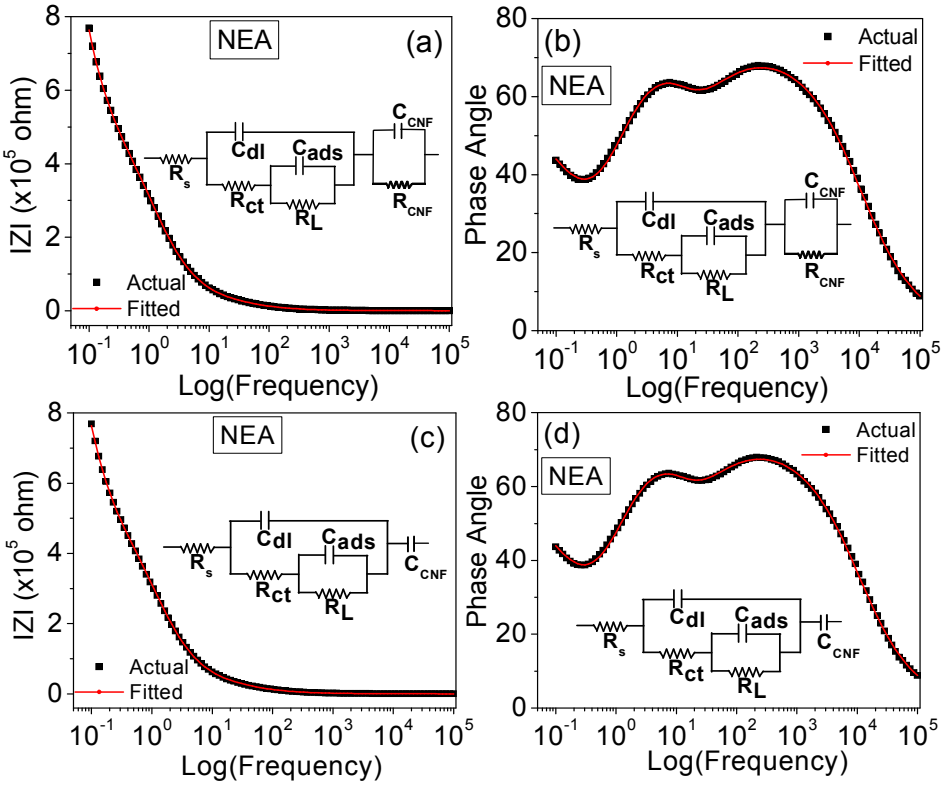

Figure S7. Bode plots of EIS of a CNF NEA functionalized with ferrocene. (a) and (c): the total impedance vs. log(frequency). (b) and (d): phase angle vs. log(frequency). These are the same EIS data shown in Nyquist plot in Figure 6(b). (a) and (b) use a parallel circuit (C_{CNF} and R_{CNF})

to represent intrinsic properties of the CNF while (c) and (d) only use a single capacitor C_{CNF}. As seen in the figure, the two equivalent circuits fit the experimental EIS data equally well.

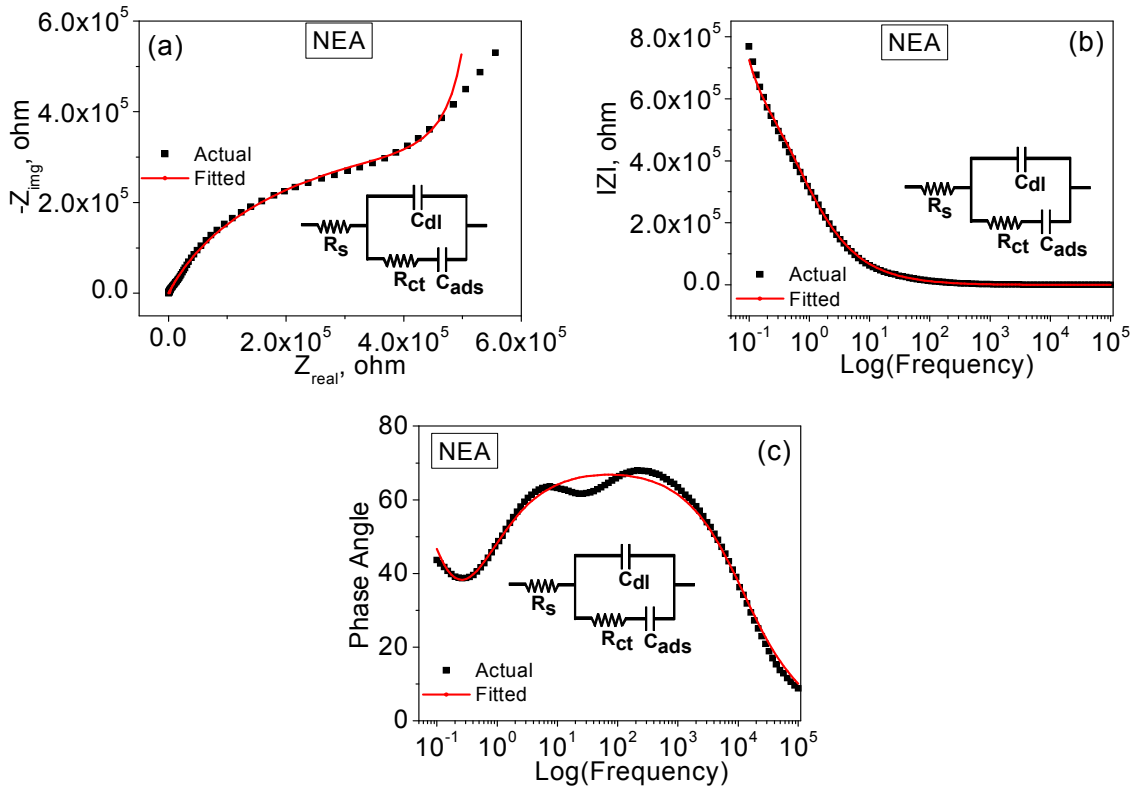

Figure S8. Nyquist (a) and Bode plots of (b) impedance vs. log(frequency) and (c) phase angle vs. log(frequency) of a CNF NEA functionalized with ferrocene, fitted with modified Randles circuit that was used by Creager [7].

Modified Randles circuit which was used by Creager et al [7] was initially tried to fit the EIS data of the ferrocene functionalized CNF NEA. The plots of which are shown in Figure S8 and it can be clearly seen that this equivalent circuit cannot fit the data very well. The unsatisfied fitting quality is more obvious when we look at the Bode plot (Figure S8(c)) of phase angle vs. log(frequency). Particularly, the two peaks at ~5 Hz and ~650 Hz indicate that the circuit should

consist of two RC circuits in series as shown in Figure 6(b). This provides strong justification to the equivalent circuit that is used (Figure 6(b) and Figure S7) to fit the EIS of the ferrocene-functionalized CNF NEA.

Table S2: Comparison of the fitting parameters of the two equivalent circuits for the electrochemical impedance spectra of Fc-attached CNF NEA electrodes

Circuit for CNF	**R_s, Ω**	**C_{dl}, F (n)**	**R_{ct}, Ω**	**C_{ads}, F (n)**	**R_L, Ω**	**C_{CNF}, F (n)**	**R_{CNF}, Ω**	**k^o_{ac} (s^{-1})**
Parallel C_{CNF}, R_{CNF}	311.3	4.144×10^{-7} (0.864)	5.167×10^{4}	2.552×10^{-7} (0.976)	2.621×10^{5}	2.488×10^{-6} (0.707)	2.946×10^{7}	**38.0**
C_{CNF} only	312.5	4.451×10^{-7} (0.85)	5.997×10^{4}	2.187×10^{-7}	2.664×10^{5}	2.561×10^{-6} (0.715)	--	**38.1**

References:

[1] A. Baramee, A. Coppin, M. Mortuaire, L. Pelinski, S. Tomavo, J. Brocard, *Bioorg. Med. Chem.* **2006**, *14*, 1294.
[2] J. Li, H. T. Ng, A. Cassell, W. Fan, H. Chen, Q. Ye, J. Koehne, J. Han, M. Meyyappan, *Nano Lett.* **2003**, *3*, 597.
[3] B. A. Cruden, A. M. Cassell, Q. Ye, M. Meyyappan, *J. Appl. Phys.* **2003**, *94*, 4070.
[4] L. Zhang, D. Austin, V. I. Merkulov, A. V. Meleshko, K. L. Klein, M. A. Guillorn, D. H. Lowndes, M. L. Simpson, *Appl. Phys. Lett.* **2004**, *84*, 3972.
[5] Q. Ngo, A. M. Cassell, A. J. Austin, J. Li, S. Krishnan, M. Meyyappan, C. Y. Yang, *IEEE Electron Device Lett.* **2006**, *27*, 221.
[6] S. Creager, C. J. Yu, C. Bamdad, S. O'Connor, T. MacLean, E. Lam, Y. Chong, G. T. Olsen, J. Y. Luo, M. Gozin, J. F. Kayyem, *J. Am. Chem. Soc.* **1999**, *121*, 1059.
[7] S. E. Creager, T. T. Wooster, *Anal. Chem.* **1998**, *70*, 4257.